NUMERICAL SIMULATION OF NATURAL CONVECTION IN SQUARE CAVITY FILLED WITH NANOFLUIDS FOR DIFFERENT THERMAL CONDUCTIVITY AND VISCOSITY MODELS

Fábio Ricardo Oliveira de Souza, fsouza.unisinos@gmail.com
Rejane de Césaro Oliveski, decesaroo@gmail.com
Ariadna Schuck, ariadnapss@gmail.com
Universidade do Vale do Rio dos Sinos - UNISINOS, Av. Unisinos, 950, São Leopoldo, RS 93022-000, Brasil.

Abstract. *The nanofluids may offer important advantages over conventional fluids for heat transfer systems. In the past decade, researchers focused on measuring the effective thermal conductivity and viscosity of nanofluids. The Natural convection inside square cavities has a variety of practical and technological applications, motive for which there is a constant concern to improve the existing knowledge. In this paper the numerical modeling is performed to simulate natural convection of Al_2O_3 nanoparticles and water base fluid in square enclosure. We consider four cases using different models of thermal conductivity and dynamic viscosity associated with the physical properties of the selected nanofluid. Simulations were performed for Rayleigh number values ranging from 10^3 to 10^6. Stable suspensions of Al_2O_3 solid nanoparticles were considered for volume fractions ranging up to 4%. Results indicate that the average Nusselt number increases and decreases according to the thermal conductivity model, particle volume concentration and Rayleigh number applied. In this work, it is presented Nusselt numbers deviations for two thermal conductivities and two dynamic viscosity models. The results were obtained by continuity, momentum and energy equations coupled using computational fluid dynamics (CFD).*

Keywords*: nanofluids, natural convection, square cavities, Al_2O_3 nanoparticle.*

1. NOMECLATURE

Cp	specific heat capacity (J/kg K)
g	gravitational acceleration (m/s²)
H	height of enclosure (m)
k	thermal conductivity (W/m K)
Nu	Nusselt number
$\overline{Nu}$	average Nusselt number
p	pressure (Pa)
Pr	Prandtl number
Ra	Rayleigh number
T	temperature (K)
u, v, w	velocity components (m/s)
V	dimensionless speed
W	width of enclosure (m)
x, y, z	Cartesian coordinates (m)
X, Y	dimensionless coordinates

Greek Symbols

α	thermal diffusivity (m²/s)
β	thermal expansion coefficient (1/K)
ϕ	particle volume fraction
μ	dynamic viscosity (kg/m s)
θ	dimensionless temperature
ρ	density (kg/m³)
υ	kinematic viscosity (m²/s)

Subscripts

bf	base fluid
c	cool
h	higher
nf	nanofluid
p	nanoparticle

2. INTRODUCTION

Nanofluids have interesting thermal properties when compared to conventional heat transfer fluids. In this case, with the addition of a small amount of nanoparticles, it occurs an increase in the thermal conductivity (Choi et al. 1998). For example, in concentrations of 4% of nanoparticles dissolved in base fluid, it is possible to increase the thermal conductivity by 25% in relation to the thermal conductivity in the base fluid. However, the thermal conductivity of nanofluids also has a temperature dependence of the operation temperature (Das et al. 2003, Choi et al. (1998).

The thermophysical properties of nanofluids may vary according to the concentration of particles and also to their shape. Several authors have tried to formulate equations that can describe the thermophysical behavior of nanofluids. Regarding the thermal conductivity, we can mention the works of Masuda et al. (1993), Choi (1995), Eastman et. Al (1997), Xuan and Li (2000), Keblinski et al. (2005) Xie et al (2002), Wang et al. (2003) and Ding and Wen (2004). Regarding the convective processes we can cite the works of Park and Cho (1999), Xuan and Roetzel (2000), Xuan and Li (2003), Ding and Wen (2004), Das et al. (2003), Tsai et al. (2003) and You et al (2003).

The thermal conductivity of nanofluids is more sensitive to temperature than the pure base fluid. Most studies confirm this trend, showing that the increase of the thermal conductivity is more significant with the increase of the temperature. For particles of Al_2O_3 and CuO dissolved in water, Das et al. (2003) showed an increase in thermal conductivity with the increase of the temperature. Minsta et al. (2009) studied the effect of temperature in the thermal

conductivity of the same nanofluids. For a range of 20 to 40 ° C there was an average increase of approximately 15% in the thermal conductivity of each type of nanofluid, while the increase for pure water in the same temperature range was only 5%.

Masuda et al. (1993) found that the viscosity of the nanofluid depends on the temperature and concentration. Furthermore, they found that there is little influence of the size of the nanoparticle, except in cases of high concentrations. Finally, different correlations have been indicated for the behavior of the viscosity of nanofluids. According to Zhang (2007), Einstein's formula and its derived expressions, originated from the classical theory of linear fluids, is useful, but limited to small volumetric concentrations of nanoparticles

The fluid thermal conductivity is one of the most influential factors in the development and use of heat transfer equipments. However, the traditional fluids used in these devices, such as water, oil or mixtures of ethylene glycol have low thermal conductivity (Choi, 1998). The conventional method to improve the heat transfer rate is to increase the area available for heat exchange. Thus, this method requires an undesired increase in size of system components. One solution for this is the use of other fluids with improved thermal performance in industrial processes (Keblinski et al., 2005). Likewise, the natural convection in the cavities is important because it reduces the use of pumps for fluid movement.

From these studies, several correlations have been developed for the thermal conductivity and for the dynamic viscosity, considering the same types and concentrations of nanoparticles. The processes of heat transfer under natural convection are influenced by the variation of thermophysical properties of the fluid under analysis. In this case, the definition of the properties of the nanofluid strongly depends on the correlations chosen, mainly for the thermal conductivity and absolute viscosity, suggested by the works previously mentioned. Thus, the objective of this study is to analyze numerically the behavior of nanofluids submitted to the process of natural convection in a square cavity. The analysis is performed with nanoparticles of aluminum oxide (Al_2O_3) dissolved in water and results are evaluated with different volume fractions and Rayleigh numbers. For each one of these conditions, different models for obtaining the thermal conductivity and dynamic viscosity of nanofluids are evaluated.

3. SIMULATION METHODOLOGY AND MATHEMATICAL MODEL

The study is conducted in a square cavity, where the horizontal walls are maintained as adiabatic and the vertical walls at fix uniform temperature as indicated in Figure 1. The temperature difference between the vertical walls causes a bouyancy force that promotes the circulation of the fluid.

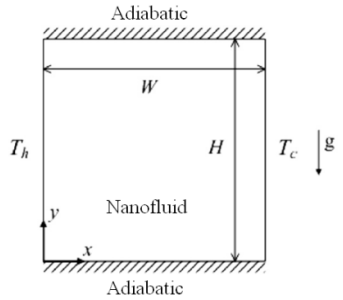

Figure 1. Schematic domain of the physical model.

where W is the width and H the height of the cavity. Th and Tc represent the high and low temperatures, respectively.

The working fluid is considered incompressible. Thus, the basic mathematical model consists of the continuity (1), the momentum (2 and 3), and energy (4) equations, which are displayed in the sequence.

$$\frac{\partial u}{\partial x}+\frac{\partial v}{\partial y}=0 \tag{1}$$

$$u\frac{\partial u}{\partial x}+v\frac{\partial u}{\partial y}=\frac{1}{\rho_{nf}}\left[-\frac{\partial p}{\partial x}+\mu_{nf}\left(\frac{\partial^2 u}{\partial x^2}+\frac{\partial^2 v}{\partial y^2}\right)\right] \tag{2}$$

$$u\frac{\partial v}{\partial x}+v\frac{\partial v}{\partial y}=\frac{1}{\rho_{nf}}\left[-\frac{\partial p}{\partial y}+\mu_{nf}\left(\frac{\partial^2 u}{\partial x^2}+\frac{\partial^2 v}{\partial y^2}\right)+\rho_{nf}\cdot\beta_{nf}\cdot g\left(T-T_m\right)\right] \tag{3}$$

$$u\frac{\partial T}{\partial x}+v\frac{\partial T}{\partial y}=\alpha_{nf}\left(\frac{\partial^2 T}{\partial x^2}+\frac{\partial^2 T}{\partial y^2}\right) \tag{4}$$

where u and v are the velocity components in x and y directions, respectively, ρ is the density, p is the pressure, T is the temperature, α is de thermal diffusivity, β is thermal expansion coefficient and μ is the dynamic viscosity. The subscript nf refers to nanofluids.

Based on Lai and Yang (2011) and Ravnik et al. (2010) works, the square cavity has sides equal to 0.01 m, stable suspensions of Al_2O_3 solid nanoparticles and water as base fluid. The Rayleigh number values applied ranging from 10^3 to 10^6 and volume fractions ranging from 1% to 4%. The physical properties of nanofluids have been estimated using classical models to mixtures of density (ρ_{nf}), specific heat capacity (Cp_{nf}), thermal expansion coefficient (β_{nf}) and thermal diffusivity (α_{nf}), Eq (5-8), respectively.

$$\rho_{nf} = (1-\varphi)\rho_{bf} + \varphi\rho_p \tag{5}$$

$$(\rho Cp)_{nf} = (1-\phi)(\rho \cdot Cp)_{bf} + \phi(\rho \cdot Cp)_p \tag{6}$$

$$(\rho \beta)_{nf} = (1-\phi)(\rho \cdot \beta)_{bf} + \phi(\rho \cdot \beta)_p \tag{7}$$

$$\alpha_{nf} = k_{nf} / (\rho \cdot Cp)_{nf} \tag{8}$$

The thermal conductivity models used are the Maxwell (1891, Eq. 9) and Angue (2009, Eq. 10). The dynamic viscosity model applied in this study are the Nguyen et al. (2009, Eq. 11) and Brinkman, Eq. (12).

$$k_{nf} = \frac{k_p + 2k_{bf} + 2\phi(k_p - k_{bf})}{k_p + 2k_{bf} - \phi(k_p - k_{bf})} k_{bf} \tag{9}$$

$$k_{nf} = (1.72\phi + 1.0)k_{bf} \tag{10}$$

$$\mu_{nf} = 0.904e^{14.8\phi}\,\mu_{bf} \tag{11}$$

$$\mu_{nf} = (1-\phi)^{-2.5}\,\mu_{bf} \tag{12}$$

where (ϕ) is the nanoparticles fractions, (Cp) is the specific heat capacity, (k) is the thermal conductivity, (μ) is the dynamic viscosity and the subscriptions p, bf, nf denote the particle, the base fluid and the nanofluid, respectively.

Fluid and nanoparticles' thermo-physical properties used are presented in Tab. 1.

Table 1. Thermo-physical properties of fluid and nanoparticles.

Property	Al_2O_3	Fluid phase (water)
density (kg/m^3)	3880	997
thermal equilibrium (J/kg K^{-1}) [a]	765	4179
thermal expansion (1/K)	0.0000085	0.00021
thermal conductivity (W m^{-1} K^{-1}) [a]	40	0.613
dynamic viscosity (kg/m s^{-1})	-	0.000855
morphology	spherical	-
particle size (nm)	47	-

[a] Reference temperature at 25°C.

The correlations for thermal conductivity (Eq. 5 and 6) and dynamic viscosity (Eq. 7 and 8) showed significant difference between the results. The tests are presented in the Tab. 2. As it can be in this table, the viscosity increases up to 10.7% with the Brinkman model when the particle fraction (ϕ) up to 4%. When this particle fraction is applied in the Nguyen model, this value increases up to 63.4%. To thermal conductivity, the maximum increase was 6.9% and 11.9% to Angue and Maxwell models, respectively.

Table 2 - Thermal conductivity and viscosity results for different models.

ϕ	k_{nf} Angue	k_{nf} Maxwell	Factor Angue	Factor Maxwell	μ_{nf} Brinkman	μ_{nf} Nguyen	Factor Brinkman	Factor Nguyen
%	(W m^{-1} K^{-1})				(kg/m s^{-1})			
0	0.6130	0.6130	-	-	8.550E-4	8.550E-4	-	-
1	0.6235	0.6307	1.017	1.029	8.768E-4	8.960E-4	1.025	1.048
2	0.6341	0.6488	1.034	1.058	8.993E-4	1.040E-3	1.052	1.215
3	0.6446	0.6673	1.052	1.089	9.227E-4	1.200E-3	1.079	1.409
4	0.6552	0.6861	1.069	1.119	9.469E-4	1.400E-3	1.107	1.634

For natural convection in the closed cavity, the dynamic similarity depends on the Prandtl number (Pr, Eq. 13) and the Rayleigh number (Ra, Eq. 14). The Nusselt number (Eq. 15) depending on the thermal conductivities of the base fluid (k_{bf}) and on the nanofluid (k_{nf}). The average Nusselt number ($\overline{Nu}$) is defined in Equation (16). The temperature and the dimensionless coordinates are defined by Equations (17-19), respectively.

$$\mathrm{Pr} = \upsilon/\alpha \tag{13}$$

$$Ra = \left(g\,\beta\,\Delta T\,H^3\right)/(\alpha\upsilon) \tag{14}$$

$$Nu = -\frac{k_{nf}}{k_{bf}}\frac{\partial\theta}{\partial X} \tag{15}$$

$$\overline{Nu} = \int_0^1 Nu\,dY \tag{16}$$

$$\theta = \left(T - T_c\right)/\left(T_h - T_c\right) \tag{17}$$

$$\mathrm{X} = \mathrm{x}/\mathrm{W} \tag{18}$$

$$Y = y/H \tag{19}$$

where υ is the kinematic viscosity and g is the gravitational acceleration, , respectively.

It was used the commercial software ANYS-CFX-12 to simulate the problem. In this, the differential equations (Eq. 1-4) are discretized and numerically solved for each point of the computational domain. The mesh used is a hexahedral type with refinement near the walls.

4. RESULTS

In order to evaluate the mesh sensitivity, we have performed computational tests with meshes of 30x30, 50x50, 150x150 and 250x250 elements. In Table 2 it is shown average Nusselt number ($\overline{Nu}$) results, obtained through these computational meshes for Rayleigh number equal to 10^6. As can be seen, the results show very little variation in Nusselt number between the mesh 3 and 4. Therefore, we chose the mesh 3 to make the simulations of all cases proposed.

Table 2 – Number of elements in the tested meshes.

Mesh	Num. of elements	$\overline{Nu}$	Variation %
1	30x30	9.533	2,49
2	50x50	9.301	0,87
3	150x150	9.220	0,34
4	250x250	9.251	- - -

The processes were simulated with different Rayleigh numbers for base fluid (water) and compared with literature results. The average Nusselt number for different cases is shown in Table 3. In this table cam be seen the good agreement between the results of this and previous works (Kahveci, 2010 and Lai and Yang, 2001).

Table 3 – Average Nusselt number $\overline{Nu}$.

Ra	Present study	Lai and Yang (2011)	Kahveci (2010)
10^3	1.114	1.128	- - -
10^4	2.235	2.286	2.274
10^5	4.656	4.729	4.722
10^6	9.220	9.173	9.230

The evaluation results of dependence of computational mesh, shown in Tab.2, and those related to the average Nusselt number, shown in Table 3, indicate that the mathematical model and computational mesh are well defined for the proposed problem (natural convection in the cavity for Rayleigh number up to 10^6). Then, simulations were conducted with pure water and nanofluids for different Rayleigh numbers. For nanofluid, various concentrations of nanoparticles of Al_2O_3 were used for each Rayleigh number. The concentrations (ϕ) of nanoparticle used were 1 and 4%.

Figures 2 (a-b) and 3 (a-b) show velocity results for pure water and nanofluid with nanoparticle concentration of 4%. The velocities (v) of Figure 2 (a-b) were evaluated at position y=H/2, while the velocity (u) of Figure 3 (a-b) were evaluated at position X=W/2.

In Figures 2(a) and 3(a) the results are for Rayleigh numbers equal to 10^5, while the results of Figures 2(b) and 3(b) are for Rayleigh numbers equal to 10^6. For the nanofluids, two models of thermal conductivity were used (Maxwell and Angue) and one dynamic viscosity model (Brinkman). In these figures can be seen that, at the minimum and maximum points, the nanofluids show higher velocity than those presented by pure water. This increase results in an increase in the heat transfer coefficient and consequently also in the average Nusselt number.

The Maxwell thermal conductivity model reaches greater velocity (v) at maximum and minimum points when compared to the Angue thermal conductivity model. The phenomenon that occurs in Figure 2 (a-b) also can be seen in Figure 3 (b), where the Maxwell model achieves greater velocities (u) at the minimum and maximum point, in relation to the Angue model.

The curves of velocities (u) and (v) of the nanofluids indicated no significant difference in relation to the results shown in Figs. 2 and 3, when the Brinkman model was replaced by the Nguyen model.

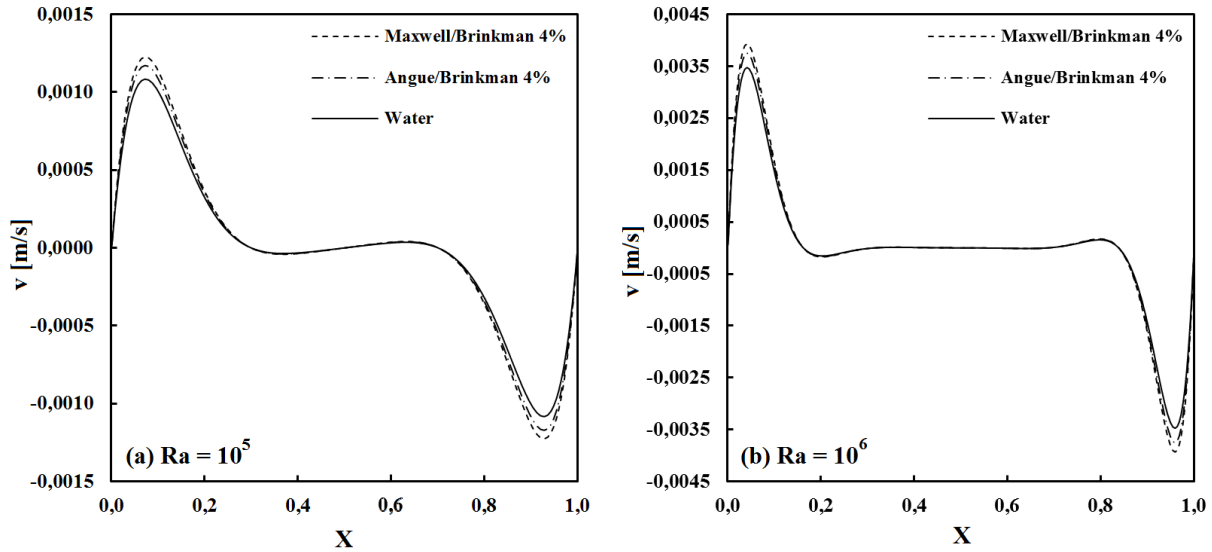

Figure 2. Velocity v: (a) Ra=10^5 (b) Ra=10^6.

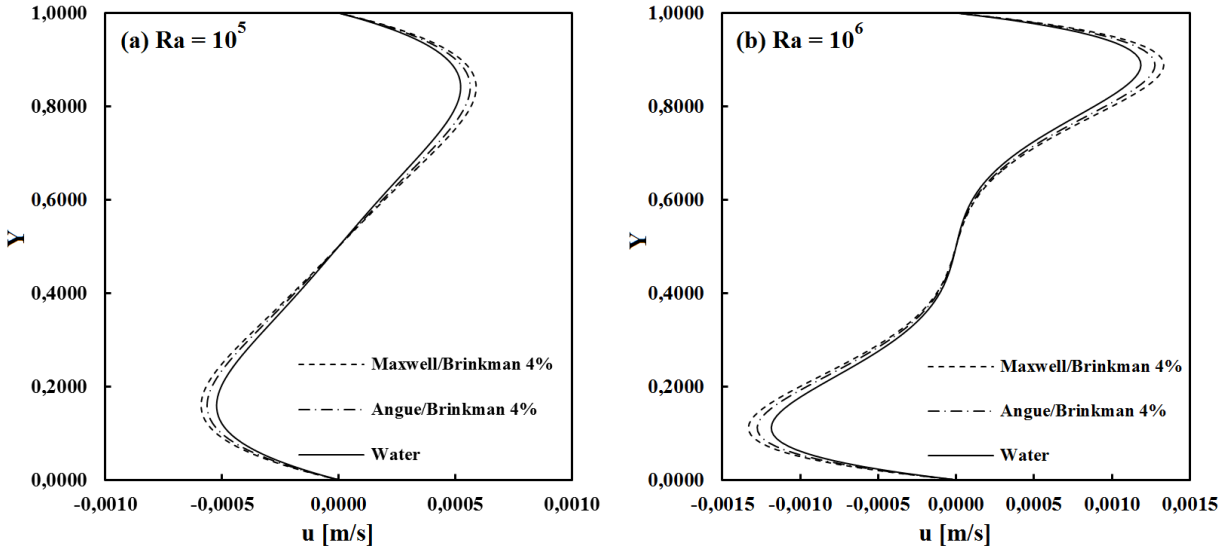

Figure 3. Velocity u: (a) Ra=10^5 (b) Ra=10^6.

Figure 4 (a-d) shows isotherms for pure water (dashed curves) and nanofluid (continuous curves) with concentration of 4% for various Rayleigh numbers. For Ra=10^3 (Fig. 4a), the isotherms are almost vertical, indicating that the heat transfer process is predominantly conductive. For Ra=10^4 (Fig. 4b), the thermal boundary layer near the vertical walls begins to decrease and the isotherm at the cavity center present inflection points. For Ra=10^5 (Fig. 4c), the

thickness of the thermal boundary layer near the wall decreases and the isotherm at the cavity center starts to become horizontal. In Ra=10^6 (Fig. 4d) the isotherm at the cavity center becomes horizontal.

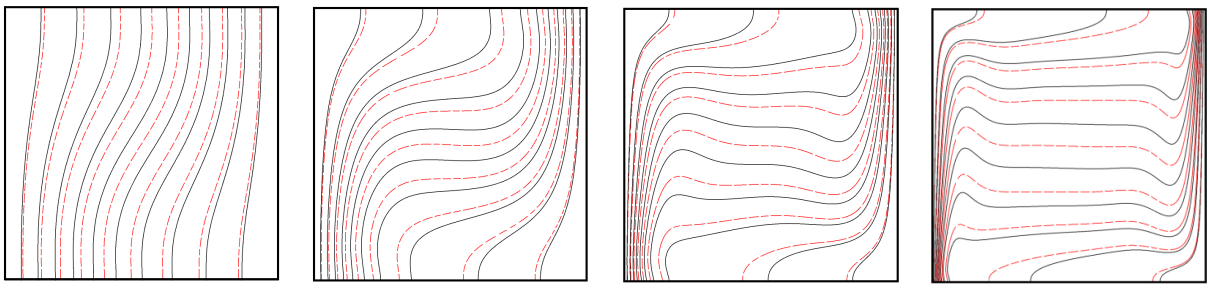

(a) (b) (c) (d)

Figure 4. Isotherms - water and nanofluid with 4% of Al_2O_3: (a) Ra=10^3, (b) Ra=10^4, (c) Ra=10^5 and (d) Ra=10^6.

Figures 5 (a-b) and 6(c-d) shows the variation of the local Nusselt number (Nu) of pure water and nanofluids with φ=1% and φ= 4%, along the hot wall of the cavity, for Ra=10^3, 10^4, 10^5 and 10^6, respectively. Initially, in these figures can be observed that the Nusselt number at the cavity base is much larger than that observed at the cavity top, because hot wall is on the right side of the cavity. In these conditions the net force is upwards. So, the direction of movement of the fluid is horary. Thus, portions of cold mass come into contact with the hot wall at the bottom, while the top of this wall is in contact with the hottest parcels of fluid. That is, at the cavity bottom, the differences in temperature between the wall and the fluid in contact with it are much greater than the differences in temperature between the top of the hot wall with the fluid at that location, causing high Nusselt numbers at the base and lowest at the top.

Regarding the various cases shown in Figure 5 (a-d), for all Rayleigh numbers, any model tested, regardless of the concentration of nanoparticles, nanofluids present Nusselt number higher than those observed for pure water. Furthermore, it is observed that nanofluids with higher concentrations present larger Nusselt number, probably due to the greater temperature difference between the wall and the fluid, associated with the increase in the thermal conductivity of the chosen mathematical model. As can be seen in Table 2, the model of thermal conductivity of Maxwell estimates larger values of k and ΔT, when compared to values of the model of thermal conductivity of Angue. In Figures 5 (a-b) and 6 (c-d) the curves of Maxwell model are higher when compared to the curves of the Angue model, especially for ϕ =4%.

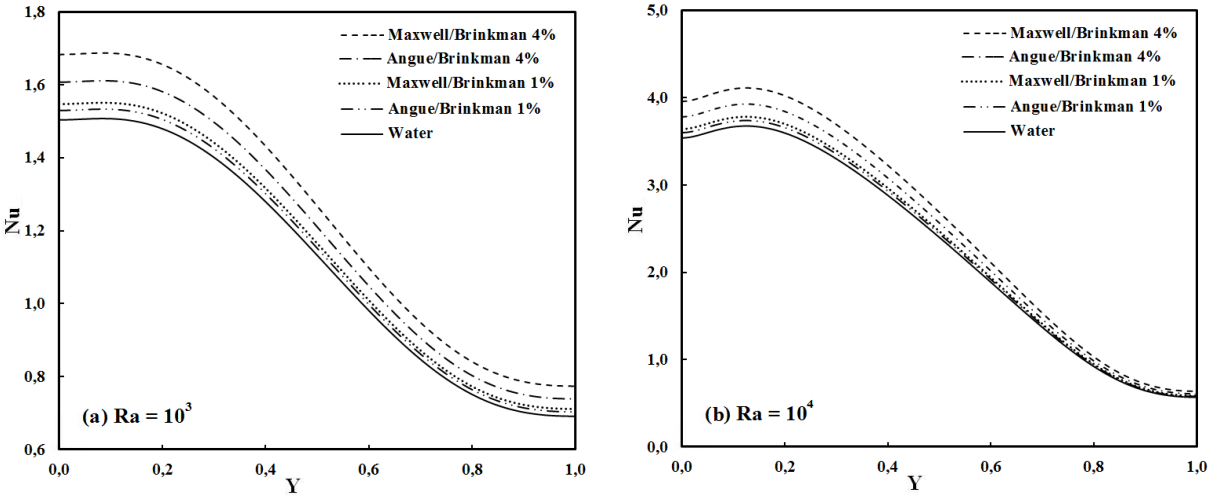

Figure 5. Local Nusselt number for different models: (a) Ra = $10^3$and (b) Ra=10^4.

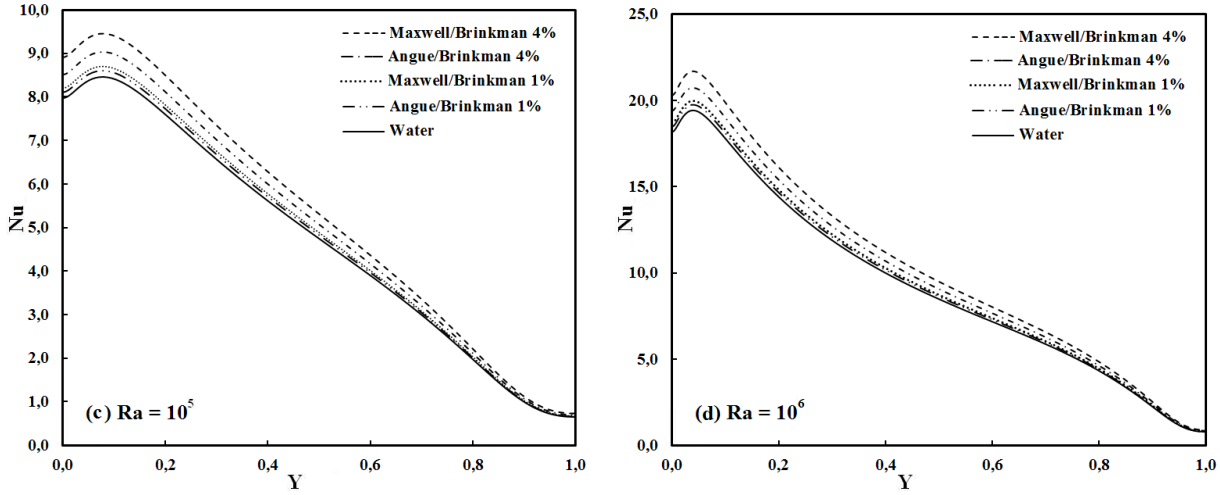

Figure 6. Local Nusselt number for different models: (c) Ra=10^5 and (d) Ra=10^6.

Table 4 shows the average Nusselt number for different Rayleigh number, particle concentrations and tested models. Regarding the thermal conductivity, the Maxwell/Brinkman model, with ϕ=4%, shows results with an increase of approximately 4.5% in the average Nusselt number, when compared with the Angue/Brinkman model, primarily for high concentrations of nanoparticles. For the dynamic viscosity, obtained by the Maxwell/Brinkman model and ϕ=4%, the results show a maximum increase of 0.15% in the average Nusselt number when compared to Maxwell/Nguyen model. The same is observed when we compare the results of Angue/Brinkman and Angue/Nguyen models.

Table 4 – Average Nusselt numbers for different Rayleigh numbers and models.

		$\overline{Nu}$						
Ra	ϕ	Maxwell Brinkman	Angue Brinkman	Relative error	Maxwell Nguyen	Relative error	Angue Nguyen	Relative error
10^3	1	1,146541	1,133553	1,133	1,146693	0,013	1,133466	1,140
	4	1,247165	1,191032	4,501	1,247152	0,001	1,190983	4,505
10^4	1	2,299727	2,273571	1,137	2,299803	0,003	2,273622	1,135
	4	2,501153	2,388647	4,498	2,502295	0,046	2,389699	4,456
10^5	1	4,790038	4,735568	1,137	4,790389	0,007	4,735922	1,130
	4	5,208385	4,974699	4,487	5,214424	0,116	4,980077	4,383
10^6	1	9,588755	9,479846	1,136	9,589687	0,010	9,480749	1,126
	4	10,425075	9,957881	4,481	10,441155	0,154	9,972267	4,343

5. C ONCLUSIONS

Natural convection process in cavity was numerically simulated by ANSYS-CFX commercial software. Different fluids were employed: pure water and nanofluids with different concentrations of nanoparticles, with Rayleigh numbers ranging from 10^3 to10^6.

The numerical model and the computational mesh were validated with results of Nusselt number found in the literature, showing excellent agreement between them.

Results were presented in terms of isotherms and Nusselt number for different concentrations of nanoparticles for different Rayleigh numbers. Through these it was found that the average Nusselt number increases with the increasing concentration of nanoparticles, and these results are always higher than those presented with pure water.

The thermal conductivity model of Maxwell estimates a higher average Nusselt number when compared to the Angue model, which indicates a strong dependence of the thermal conductivity model applied.

The dynamic viscosity model applied show little variation to the maximum concentration of tested nanoparticles, indicating a low dependence of the dynamic viscosity model applied.

6. REFERENCES

Choi, S. U. S., 1998. *Nanofluid technology: Current Status and Future Research.*, Korea-U.S. Technical Conference on Strategic Technologies, Vienna, VA (US).

Choi S.U.S., Eastman J.A., 1995. Enhancing Thermal Conductivity of Fluids with Nanoparticles. *In Proceedings Of The 1995 ASME International Mechanical Engineering Congress and Exposition,* San Francisco, CA, USA.

Das, S. K., Putra, N., Thiesen, P., Roetzel, W., 2003. "Temperature Dependence of Thermal Conductivity Enhancement for Nanofluids". *Journal of Heat Transfer*, Vol. 125, pp. 567-574.

Eastman, J. A., Choi, S. U. S., LI, S., Thompson, L. J., Lee, S., 1996. *Enhanced Thermal Conductivity Through the Development of Nanofluids*. Materials Research Society Symposium - Proceedings, Nanophase and Nanocomposite Materials II, Vol. 457, pp. 3-11.

Keblinski, P., Eastman, J. A., Cahill, D. G, 2005. *Nanofluids for Thermal Transport*. Materials Today, Vol. 8, pp. 36-44.

Masuda H., Ebata, A., Teramae, K. & Hishinuma, N.. 1993. Alteration of Thermal Conductivity and Viscosity of Liquid by Dispersing Ultra-Fine Particles (dispersion of c-Al2O3, SiO2 and TiO2 ultra-fine particles). *Netsu Bussei* (Japan), Vol. 4, pp. 227–233.

Minsta H.A., Roy G., Nguyen C.T., Doucet D., 2009. New Temperature Dependent Thermal Conductivity Data for Water-Based Nanofluids. *International Journal of Thermal Sciences*, Vol. 48, pp. 363-371.

Pak B.C., Cho Y.I., 1998,"Hydrodynamic and heat transfer study of dispersed fluids with submicron metallic oxide particles", *Experimental Heat Transfer*, Vol. 11, pp. 151- 170.

Tsai C.Y., Chien, H.T., Ding, P.P., Chan, B., Luh, T.Y., & Chen, P.H., 2004, "Effect of Structural Character of Gold Nanoparticles in Nanofluid on Heat Pipe Thermal Performance." *Materials Letters*., Vol. 58, pp. 1461–1465.

Wen D.S., Ding, Y.L., 2004. Experimental Investigation into Convective Heat Transfer of Nanofluids at the Entrance Area under Laminar Flow Conditions. *International Journal of Heat and Mass Transfer*, Vol. 47, pp. 5181– 5188.

Wang B.X., Zhou, L.P., Peng, X.F., 2003. Fractal Model for Predicting the Effective Thermal Conductivity of Liquid with Suspension of Nanoparticles. *International Journal of Heat and Mass Transfer*, Vol. 46, p. 2665–2672.

Xie H., Wang, J., Xi, T.G., Liu, Y., Ai, F., 2002. Thermal Conductivity Enhancement of Suspensions Containing Nanosized Alumina Particles. *Journal of Applied Physics*, Vol. 91, p. 4568–4572.

Xuan Y.M., Roetzel, W., 2000, "Conceptions for Heat Transfer Correlation of Nanofluids", *International Journal of Heat and Mass Transfer*, Vol. 43, pp. 3701– 3707.

Xuan, Y., Li, Q., 2000. Heat Transfer Enhancement of Nanofluids. *International Journal of Heat and Fluid Flow*, Vol. 21, pp. 58-64.

Xuan, Y., Li, Q., 2003. Investigation on Convective Heat Transfer and Flow Features of Nanofluids. *ASME Journal of Heat Transfer*, Vol. 125, pp. 151–155.

You S.M.,. Kim, J.H. & K.H. Kim., 2003."Effect of Nanoparticles on Critical Heat Flux of Water in Pool Boiling Heat Transfer.", *Applied Physics Letters*, Vol. 83, pp. 3374–3376.

Zhang, Z. M. Nano/microscale Heat Transfer. New York: McGraw Hill, 2007.

7. RESPONSIBILITY NOTICE

The authors Fábio Ricardo de Oliveira de Souza, Rejane de Césaro Oliveski and Ariadna Schuck are the only responsible people for the printed material included in this paper.

8. ACKNOWLEDGMENTS

The authors acknowledge the financial support of CNPq - Conselho Nacional de Desenvolvimento Científico e Tecnológico do Brasil (National Council for Scientific and Technological Development of Brazil) and CAPES - Coordenação de Aperfeiçoamento de Pessoal de Nível Superior (Coordination for the Improvement of Higher Education Personnel).